The triple-Q-spin-density wave in the face-centred cubic antiferromagnetic $Fe_{54}Mn_{46}$ alloy

1990 J. Phys.: Condens. Matter 2 5747

(http://iopscience.iop.org/0953-8984/2/26/011)

J. Phys.: Condens. Matter 2 (1990) 5747–5752. Printed in the UK

The triple-Q spin-density wave in the face-centred cubic antiferromagnetic $Fe_{54}Mn_{46}$ alloy

S Kawarazaki†, Y Sasaki‡, K Yasuda†, T Mizusaki‡ and A Hirai‡

† Department of Physics, Faculty of Science, Osaka University, 560 Toyonaka, Osaka, Japan

‡ Department of Physics, Faculty of Science, Kyoto University, 606 Sakyo-ku, Kyoto, Japan

Received 25 September 1989, in final form 15 January 1990

Abstract. The method of anisotropy measurement of γ-ray emission from spin-polarised nuclei has been applied to the FCC $Fe_{54}Mn_{46}$ alloy to deduce the ground-state magnetic structure. Measurements were made at temperatures down to 240 μK, and the observed anisotropy of the emission from ^{54}Mn isotopes embedded in the single-crystal sample gives definitive evidence for the triple-Q spin-density wave in this material.

1. Introduction

Many experimental studies [1–5] have been made on the magnetic properties of antiferromagnetic Fe–Mn alloys with FCC structure. However, it appears that there still remains some confusion in the interpretation of the antiferromagnetism of this alloy system. This confusion is mainly caused by the difficulty in determining experimentally the ground-state magnetic structure of the system. Figure 1 shows the magnetic phases in the Fe–Mn alloy system proposed by Endoh and Ishikawa [2]. All the phases in the figure are clearly distinguished from each other according to the behaviour of the Néel temperature, the average sublattice moment and the Fe hyperfine field. As is shown in the figure, the spin configurations of phases II and III are identified as non-collinear and collinear, respectively. The collinear spin structure is described as a spin-density wave (SDW) of the zone boundary mode with longitudinal polarisation and is called the single-Q SDW (S-SDW), while the non-collinear structure, which is a superposition of the three orthogonal S-SDWs, is called the triple-Q SDW (T-SDW). As has been pointed out by Kouvel and Kasper [6], the neutron diffraction method does not distinguish between the T-SDW in a crystal and the three orthogonal S-SDWs with equal populations of the magnetic domains. It should be noted that the magnetic structure of the phase II in figure 1 proposed by Endoh and Ishikawa is not based on an experiment which can unequivocally distinguish it from the other.

Some studies made on the phase II alloys have given conclusions which are contradictory to each other: Tajima *et al* [3] have measured spin-wave scattering of neutrons from $Fe_{0.7}Mn_{0.3}$ and $Fe_{0.5}Mn_{0.5}$ crystals. They observed isotropic dispersions and q-dependent damping of the spin waves and showed that these phenomena are inconsistent with the localised model of the 3D electrons but are favourable to the itinerant-electron model of Asano and Yamashita [7] where the multiple-SDW state is assumed to exist. On

0953-8984/90/265747 + 06 $03.50

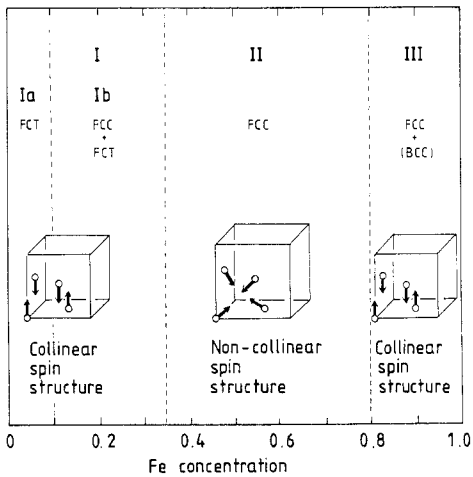

Figure 1. Magnetic phases in the Fe–Mn alloy system proposed by Endoh and Ishikawa [2].

the other hand, Bisanti *et al* [4] made a similar spin-wave experiment on the $Fe_{65}Mn_{35}$ crystal and obtained results consistent with those of Tajima *et al* but drew a contrary conclusion: according to the theory of Jensen and Bak [8], the magnon of the T-SDW has both a transverse mode (T mode) and a longitudinal mode (L mode), and the latter occupies the low-lying level at the zone centre, while the magnon of the S-SDW has only the T mode. Therefore, if a low-lying mode is observable at both the 110 and 100 zone centres, it can be evidence of the S-SDW because only the T-mode magnons are so observable. Bisanti *et al* claim the S-SDW in their crystal because they observed a mode at both 110 and 100.

At the same time as the paper of Bisanti *et al* appeared, Kennedy and Hicks [5] reported the results of their study on the $Fe_{55}Mn_{45}$ alloy and concluded the existence of the non-collinear structure in this alloy. They showed theoretically that the Mössbauer spectra of ^{57}Fe in the S-SDW and the T-SDW or the double-$\boldsymbol{Q}$ SDW (D-SDW) (to be explained later) in a single-crystal sample in a strong magnetic field should be different from each other and obtained the best fit of the experimental data to the calculated Mössbauer spectrum for the T-SDW. In their method, the calculated spectra for the three spin structures look quite similar to each other and one has to make a quantitative analysis of the experimental data by adjusting many fitting variables.

Recently, we have demonstrated [9] that the method of anisotropy measurement of the γ-ray from spin-polarised nuclei is very useful to resolve the problem of the multiple-SDW and obtained direct evidence for the T-SDW in $Mn_{72}Ni_{28}$ alloy. Because the anisotropy of the γ-ray emission from the S-SDW and the T-SDW have opposite signs, one can distinguish with no ambiguity between two spin structures simply by observing the qualitative behaviour of the intensity of the emission.

In order to give a definitive answer to the question about the contradictory explanations of the spin structure of the phase II of Fe–Mn, we have applied this method to $Fe_{54}Mn_{46}$ alloy.

2. Experimental details

A ^{54}Mn isotope undergoes an electron-capture decay and emits in succession a γ-photon at 0.834 83 MeV. This emission is of E_2 type (electric quadrupole emission) and the normalised intensity pattern of the emission is represented as [10]

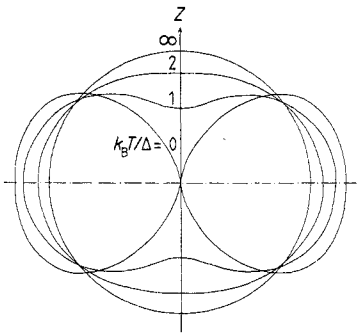

Figure 2. The angular emission pattern of γ-photons from ^{54}Mn for several temperatures. Δ is the magnitude of Zeeman splitting of the nuclear sublevels.

$$W(\theta) = 1 + \sum_{k}^{2,4} B_k U_k F_k P_k(\cos\theta) \tag{1}$$

where θ is the angle between the direction of the emission and the spin-quantising axis. The B_k-values are the kth moments of the nuclear spin direction which is determined by the magnitude of the spin polarisation, i.e. in the present case by the magnitude of the hyperfine field and the temperature. The U_k-values and F_k-values are known constants which are characteristic of the particular emission, and the P_k-values are normalised Legendre polynomials. In figure 2 is shown the calculated pattern of $W(\theta)$ as a function of Δ/k_BT, where Δ is the magnitude of the Zeeman splitting of the nuclear sublevels.

The emission pattern from the antiferromagnetically aligned nuclei in a crystal is calculated by averaging $W(\theta)$ over all the possible directions of the hyperfine fields. In figure 1, one can see that the possible directions of the spins are $\langle 100\rangle$ (all the directions which are crystallographically equivalent to [100]) for the S-SDW phase with three equally populated domains and $\langle 111\rangle$ for the T-SDW phase. In each case the probabilities of having each direction are equal to each other. Then with α_1, α_2 and α_3 the direction cosines of the direction of observation, the normalised intensity patterns from the respective phase are represented as

$$W_S(\alpha_1\alpha_2\alpha_3) = (1 + \tfrac{7}{12}B_4U_4F_4) - \tfrac{35}{12}B_4U_4F_4(\alpha_1^2\alpha_2^2 + \alpha_2^2\alpha_3^2 + \alpha_3^2\alpha_1^2) \tag{2}$$

$$W_T(\alpha_1\alpha_2\alpha_3) = (1 - \tfrac{7}{18}B_4U_4F_4) + \tfrac{35}{18}B_4U_4F_4(\alpha_1^2\alpha_2^2 + \alpha_2^2\alpha_3^2 + \alpha_3^2\alpha_1^2) \tag{3}$$

where we assumed that the direction of the hyperfine field is parallel (or antiparallel) to that of the electronic polarisation. As has been mentioned before, the anisotropy terms in W_S and W_T have opposite signs. The functions W_S and W_T have extrema at $\langle 100\rangle$ and $\langle 111\rangle$ directions. In figure 3, we show the calculated intensity of emission in the (001) plane between [100] and [110] directions for several temperatures. One can see that in the (001) plane the emission intensity has a maximum in the [110] direction and a minimum in the [100] direction for the S-SDW structure and vice versa for the T-SDW structure. In fact, [110] is not the direction of the extremum of W but that of the saddle point.

The Zeeman splitting Δ of the nuclear sublevels is caused by the hyperfine field from the polarised electronic moment and, in the case of ^{54}Mn, Δ is given as $\Delta/k_B = g_N\mu_N H_{hf}/k_B = 0.0403H_{hf}$ (mK), where g_N is the nuclear g-factor, μ_N is the nuclear magneton, and the hyperfine field H_{hf}, is measured in units of kilooersteds. The hyperfine fields at Mn nuclei in the Fe–Mn alloy system have been measured at low temperatures by Takenaka and Asayama [11] by means of NMR and have a broad spectrum between 50 and 100 kOe. The centre of gravity of the spectrum for $Fe_{54}Mn_{46}$ alloy is estimated to be 70 kOe. The splitting of the nuclear sublevels of ^{54}Mn due to the hyperfine field of 70 kOe is $\Delta/k_B =$

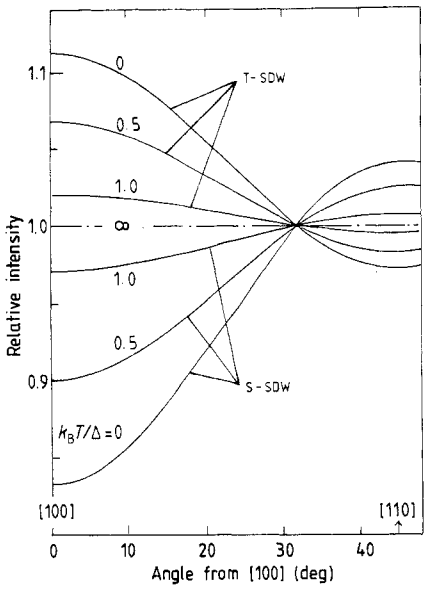

Figure 3. The normalised emission intensity in the (001) plane between [100] and [110] directions calculated for ^{54}Mn nuclei in the S-SDW and T-SDW.

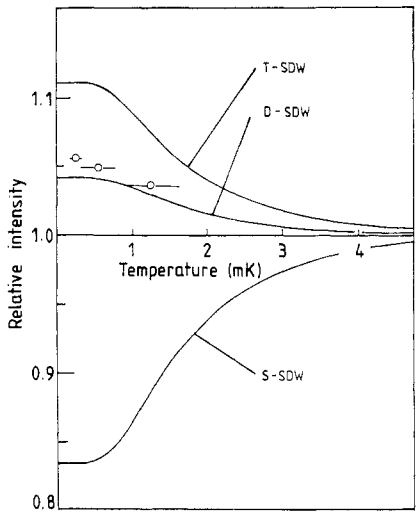

Figure 4. The normalised emission intensity in the [100] direction as a function of temperature calculated for ^{54}Mn nuclei in the $Fe_{54}Mn_{46}$ alloy: ○, observed intensities.

2.8 mK. In figure 4 is shown the temperature dependence of the emission at the [100] direction calculated for this value of Δ. In [11], the NMR spectra of $Fe_{60}Mn_{40}$ and $Fe_{50}Mn_{50}$ are given and the shape of both of these are very close to a symmetric triangle. Their width (FWHM) is about 10 kOe. Then, we calculated the effect of the broadness of the distribution of the hyperfine fields using a symmetric triangle to approximate the spectrum and found that the effect on the curve in figure 4 is very small (less than the statistical error in the measurements).

An alloy with a nominal composition of $Fe_{50}Mn_{50}$ was prepared from iron and manganese elements of 99.99% purity using an induction furnace. A single crystal was grown by the Bridgman method with use of a recrystallised alumina crucible. Part of the single crystal was chemically analysed, and the composition was 54.4 at.% Fe and 45.6 at.% Mn. From the magnetic phase diagram given by Endoh and Ishikawa [2], the Néel temperature of this alloy is estimated to be 490 K. The size of the single crystal used for the experiment was 8 mm × 5 mm × 1 mm. Using this crystal we measured the intensities of the magnetic Bragg scattering of neutrons at the magnetic reciprocal lattice points 011, 101 and 110, which correspond to the three orthogonal SDWs with wavevectors of $(2\pi/a)(100)$, $(2\pi/a)(010)$ and $(2\pi/a)(001)$, respectively, a being the lattice constant, and confirmed that all the intensities were equal to each other within the experimental error. Both the S-SDW model with three equally populated domains and the T-SDW model are consistent with this observation.

About 2 μCi of $^{54}MnCl_2$–hydrochloric acid solution was spread over a side of the sample. Annealing was carried out for 1 d at 640 °C and then for 2 d at 980 °C. During the anneal the sample was held between two plates of high-purity alumina to minimise the evaporation of manganese. After the anneal the radioactivity of the sample was about 1 μCi. Slight polishing of the surface of the sample made little change in the radioactivity, which indicates that the ^{54}Mn isotopes have diffused well into the crystal lattice.

Table 1. Observed emission intensity as a function of temperature and direction of observation. The relative intensity is normalised at the warmest counts for each direction.

Direction	Temperature (mK)	Integrated intensity	Relative intensity	Statistical error
[100]	20	669 933	100	0.24
[100]	1.8–15	674 197	100.64	0.24
[100]	0.78–1.7	694 328	103.64	0.24
[100]	0.3–0.78	702 718	104.89	0.24
[100]	0.24	706 752	105.50	0.24
[110]	30–15	559 883	100	0.26
[110]	0.26–0.3	550 893	99.03	0.26

The sample was soldered to a Ni-plated copper sample holder with $Cd_{50}In_{50}$ solder using an ultrasonic soldering iron. The purpose of the Ni plating is to break the superconductivity of the solder by the ferromagnetism of nickel and to improve its thermal conductivity. Then the sample holder was screwed onto the copper nuclear demagnetisation (ND) stage. Because it was very difficult to measure the temperature of the sample directly, we monitored the temperature of the ND stage with use of a Pt NMR thermometer. The γ-photons were counted at a distance of about 20 cm from the sample using a pure germanium solid state detector and a multichannel pulse height analyser. Although the change in the emission intensity with decreasing temperature is expected to be larger in the [111] direction than in the [110] direction, we made measurements in the [100] and [110] directions because of limitation of the space for the detector.

It took about 1 d for each measurement at a temperature. The half-decay time of ^{54}Mn is 312 d, and the emission decays by 0.22% d^{-1}. The measured integrated intensity of the emission peak was corrected for this natural decay. The detector has a solid angle of about $2 \times 10^{-2}\,\pi$ sr over the sample and this gives an error in the counting rate when compared with the calculated intensity. This error depends on the temperature and the direction of observation and is at most 0.5%; hence we did not make a correction for this error.

3. Results and discussion

The results of the experiment are shown in table 1, where one can see that in the [100] direction the integrated intensity increases steadily with decreasing temperature. At 0.24 mK, the lowest attainable temperature, the intensity is larger by 5.5% than that at 20 mK where the nuclear spins are supposed to be polarised very little. The statistical error for each integrated intensity was 0.12% (0.24% for the relative intensity) and is much smaller than this change. On the other hand, the emission rate in the [110] direction at 0.26–0.3 mK was less by 0.97% than the warm counts. This change is also significantly larger than the statistical error. The ratio of the changes in the intensity in the [100] and [110] directions is consistent with the calculation shown in figure 3.

These observations eliminate the possibility of the S-SDW and support the conclusion of the Mössbauer study [5]. Besides the S-SDW and the T-SDW described above, Kennedy and Hicks [5] have tested the possibility of the ⟨100⟩ structure which is also compatible with the neutron diffraction result. This structure has a tetragonal symmetry and two orthogonal SDWs on the *c* plane couple to one another to form the D-SDW. Corresponding

to the three tetragonal axes, a sample would have to consist of three orthogonal magnetic domains. The Mössbauer experiment [5] did not distinguish between the D-SDW and the T-SDW. The observed equal intensities of the three {110} Bragg reflections of neutrons indicate that these magnetic domains would have to be equally populated. In this case the electronic moments point in the ⟨110⟩ directions and the probabilities of finding the moments in each ⟨110⟩ direction are equal to each other. Then the normalised average of $W(\theta)$ is calculated as

$$W_D(\alpha_1\alpha_2\alpha_3) = (1 - \tfrac{7}{48}B_4U_4F_4) + \tfrac{35}{48}B_4U_4F_4(\alpha_1^2\alpha_2^2 + \alpha_2^2\alpha_3^2 + \alpha_3^2\alpha_1^2). \quad (4)$$

The functional behaviour of W_D is qualitatively the same as that of W_T, but the amplitude of the anisotropy is less in W_D. At 0 K in the [100] direction, W_T is larger by 11.1% than the high-temperature value, while W_D is so by only 4.2%. It should be noted that the observed change in the counting rate of 5.5% at 0.24 mK in the [100] direction already exceeds this possible maximum change in W_D at 0 K by much more than the statistical error (see figure 4, where the observed intensities at the lowest three temperatures are shown). This fact eliminates the possibility of the D-SDW, too, and hence gives definitive evidence that the magnetic structure realised in our sample is the T-SDW.

We have no good explanation about the conclusion of Bisanti *et al*. However, in the case of measurement of phonons in alloys by neutron scattering, it is often the case that the T-mode phonons are observable even when the spectrometer is arranged to pick up only the L-mode phonons, i.e. when the scattering vector is parallel to the phonon wavevector. Thus, separation of the L- and T-mode phonons is not very strict in the case of alloys. There may be a similar situation in the case of magnons in alloys.

Figure 4 predicts a change in the emission of about 11% for the T-SDW at 0.24 mK. The observed change of 5.5% is considerably less than this value. This disagreement is not explained by either the error due to the solid angle of the detector over the sample or the distribution of the hyperfine field which have been detected by the NMR experiment [11]. Although a temperature difference of 1.3 mK between the ND stage and the sample can explain the disagreement, we rather consider that this is due to the fluctuation of the spin structure from the perfect T-SDW caused by the chemical disorder of the crystal.

Figure 1 shows that phase III has an S-SDW structure, which has a tetragonal symmetry, on the cubic crystal lattice. A careful x-ray measurement [12] on a single crystal of $(Fe_{85}Mn_{15})_{95}C_5$ alloy has detected no tetragonality at low temperatures. The coexistence of the tetragonal spin structure and the cubic crystal structure is a matter of interest and is our next target of study by means of anisotropic γ-ray emission.

References

[1] Umebayashi H and Ishikawa Y 1966 *J. Phys. Soc. Japan* **21** 1281–94
[2] Endoh Y and Ishikawa Y 1971 *J. Phys. Soc. Japan* **30** 1614–27
[3] Tajima K, Ishikawa Y, Endoh Y and Noda Y 1976 *J. Phys. Soc. Japan* **41** 1195–203
[4] Bisanti P, Mazzone G and Sacchetti F 1987 *J. Phys. F: Met. Phys.* **17** 1425–35
[5] Kennedy S J and Hicks T J 1987 *J. Phys. F: Met. Phys.* **17** 1599–604
[6] Kouvel J S and Kasper J S 1963 *J. Phys. Chem. Solids* **24** 529–36
[7] Asano S and Yamashita J 1971 *J. Phys. Soc. Japan* **31** 1000–15
[8] Jensen J and Bak P 1981 *Phys. Rev.* B **23** 6180–3
[9] Kawarazaki S, Fujita K, Yasuda K, Sasaki Y, Mizusaki T and Hirai A 1988 *Phys. Rev. Lett.* **61** 471–4
[10] Berglund P M, Collan H K, Ehnholm G J, Gylling R G and Lounasmaa O V 1972 *J. Low Temp. Phys.* **6** 357–83
[11] Takenaka H and Asayama K 1973 *J. Phys. Soc. Japan* **35** 734–9
[12] Tsunoda Y private communication